

Minimum switching control for systems of coupled double integrators

Andrea Garulli, Antonio Giannitrapani, Mirko Leomanni
Dipartimento di Ingegneria dell'Informazione, Università di Siena
Via Roma, 56 - 53100 Siena, Italia
E-mail: {garulli,giannitrapani,leomanni}@dii.unisi.it

Abstract

This paper studies the minimum switching control problem for a system of coupled double integrators with on-off input signals, in the presence of a constant disturbance term. This type of problem is relevant to a variety of applications in which the number of transitions of on-off actuators must be minimized, in order to prevent actuator wear. Two solutions are presented in terms of steady state limit cycles. The first one provides an analytic upper bound to the maximum number of transitions per input signal. The second solution exploits the relative phases of the trajectories of the state variables, thus providing a less conservative upper bound. Additionally, a control law is presented, which steers the system in finite time to the previously derived limit cycles. The proposed techniques are demonstrated on a spacecraft attitude control application.

1 Introduction

Control systems based on switching are widely employed in a number of different contexts. While it is well-known that switching controllers provide advantages over standard controllers even for simple SISO LTI systems (see e.g., [1, 2]), one of the main motivations for resorting to switching control schemes comes from limitations in the available control actuators. Indeed, it is often the case that controllers can deliver only quantized signals or even binary signals, which significantly limits the control authority [3]. A typical behavior of switching control systems consists of limit cycle oscillations. Existence conditions and stability results for limit cycles in relay SISO systems have been widely investigated (see [4] and references therein). The analysis turns out to be much more involved when dealing with MIMO systems,

although some contributions are available in the literature [5, 6, 7]. Recently, the study of limit cycles has been extended to more general classes of switching systems, such as piecewise affine systems or hybrid systems [8, 9, 10]. Limit cycles are an acceptable solution only if they comply with the limitations imposed by the actuators. In particular, in several applications the number of input transitions must be kept as low as possible, in order to minimize wear and thus increase the actuator lifetime. A typical approach consists in the formulation of an optimal control problem, in which the performance index includes the number of input transitions. Recent examples of these approaches can be found in different application fields: power electronics [11], air conditioning systems [12], boiler control systems [13], attitude control [14]. Unfortunately, in all these cases the resulting minimum switching control problem can be approached only via numerical techniques.

Explicit solutions to minimum switching control problems are available only for some special classes of systems, a notable example being on-off control of the double integrator subject to a constant disturbance term. In this case, the limit cycle corresponding to the fuel/switch-optimal periodic solution has been fully characterised since long time [15]. However, for MIMO systems, the problem becomes very challenging even for simple dynamics, such as the case of coupled double integrators. This problem is of special interest in the context of multi-axis attitude control problem, when non orthogonal thruster configurations are adopted. In particular, if on-off low-thrust actuators are employed, the minimization of the frequency of thruster firings becomes a key technological requirement [16].

In this paper, the minimum switching control problem for a multivariable system consisting of n coupled double integrators, subject to a constant disturbance term and controlled by n on-off actuators, is addressed. The first contribution of the paper is an upper bound to the minimum switching frequency required to satisfy the state constraints. Then, a less conservative solution is found by solving a suitable optimization problem which exploits the further degrees of freedom provided by the relative phases of the periodic trajectories. The last contribution is a control law which drives the system in finite time to the periodic trajectories corresponding to the two solutions previously obtained. The advantages of the proposed approach, with respect to a model predictive control (MPC) scheme, are demonstrated on a geostationary spacecraft attitude control application.

The paper is organized as follows. Section 2 reviews known results on the minimum fuel and minimum switching control problems for a single-input double integrator. Section 3 extends the control problem to a system of

coupled double integrators, and presents two different suboptimal solutions. In Section 4, a feedback control law is derived to steer the system in finite time to the above periodic trajectories. The attitude control application is presented in Section 5, while some concluding remarks are given in Section 6.

2 Single-input problem

In this section the minimum fuel and minimum switching control problems are reviewed for a single-input double integrator with a constant disturbance term. Consider the system

$$\ddot{x}(t) = u(t) + k, \quad (1)$$

where

$$u(t) \in \{-1, 0, 1\}, \quad (2)$$

and $k > 0$ is a known constant disturbance term, such that $k < 1$ to ensure controllability of the system. The objective of the control system is to guarantee that $x(t)$ satisfies

$$|x(t)| \leq \delta, \quad \forall t \geq \bar{t}, \quad (3)$$

for some $\bar{t} \geq 0$, where δ is a known bound. Then, the minimum fuel control problem can be formulated as

$$\begin{aligned} \min_u \quad & J_f(u) = \lim_{T \rightarrow \infty} \frac{1}{T} \int_0^T |u(t)| dt \\ \text{s.t.} \quad & (1), (2), (3). \end{aligned} \quad (4)$$

The following proposition is a standard result from optimal control theory [17].

Proposition 1 *A minimizer of problem (4) satisfies*

$$u(t) \in \{-1, 0\}. \quad (5)$$

Moreover, $\min_u J_f(u) = k$.

Notice that any input sequence satisfying (5), and guaranteeing that (3) holds, is a fuel-optimal solution. A fuel-optimal control law for system (1) is

$$u(t) = \begin{cases} -1 & \text{if } s(x, \dot{x}) > 0 \text{ or } s(x, \dot{x}) = 0 \text{ and } \dot{x} > 0 \\ 0 & \text{if } s(x, \dot{x}) < 0 \text{ or } s(x, \dot{x}) = 0 \text{ and } \dot{x} < 0, \end{cases} \quad (6)$$

where the switching function $s(x, \dot{x})$ is given by

$$s(x, \dot{x}) = \begin{cases} x - \frac{1}{2(k-1)} \dot{x}^2 & \text{if } \dot{x} \geq 0 \\ x - \frac{1}{2k} \dot{x}^2 & \text{if } \dot{x} < 0. \end{cases} \quad (7)$$

Such a control law guarantees that the trajectory of the closed-loop system converges to the origin in finite time, from any initial condition. Hence, it also enforces (3) indefinitely and therefore it solves problem (4). However, an infinite switching frequency is required to keep the trajectory of system (1) exactly at the origin, which translates into undesirable chattering of the actuators in practical implementations.

Among all the fuel-optimal input sequences, finding the one which minimizes the average number of input transitions amounts to solving the problem

$$\begin{aligned} \min_u \quad & J_s(u) = \lim_{T \rightarrow \infty} \frac{1}{T} \int_0^T |\dot{u}(t)| dt \\ \text{s.t.} \quad & (1), (3), u(t) \in \{-1, 0\}. \end{aligned} \quad (8)$$

The solution to (8) can be found by using phase plane arguments. From (3) and (5), it follows that fuel-optimal state trajectories are bounded paths switching between the curves

$$\psi^L = \{(x, \dot{x}) : x - \frac{1}{2k} \dot{x}^2 = -\delta, \quad -\delta \leq x < \bar{x}\}, \quad (9)$$

$$\psi^U = \{(x, \dot{x}) : x - \frac{1}{2(k-1)} \dot{x}^2 = \delta, \quad \bar{x} \leq x \leq \delta\}, \quad (10)$$

where $\bar{x} = \delta(1 - 2k)$ (see Fig. 1). The following result characterizes the solution to problem (8) [15].

Proposition 2 *Every optimal solution $u^*(t)$ of problem (8) is such that the resulting trajectory satisfies $(x, \dot{x}) \in \psi^U \cup \psi^L$ for all $t \geq \tilde{t}$, for some $\tilde{t} \geq 0$. Moreover, the resulting minimum switching frequency is $J_s(u^*) = 2\sqrt{\gamma/\delta}$, where $\gamma = k(1 - k)/16$.*

Proposition 2 provides a minimum switching and fuel-optimal solution for system (1), under the constraints (2) and (3), in terms of a limit cycle in the phase plane. This result will be exploited in the next section, to parameterize the solutions of the multi-input minimum switching control problem, for a system of coupled double integrators.

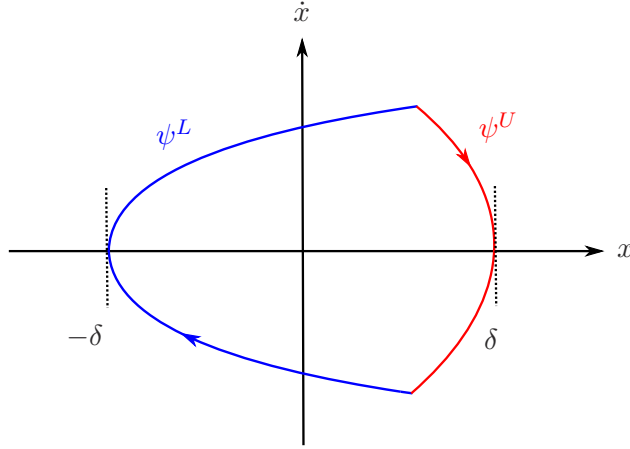


Figure 1: Fuel/switch-optimal solution to problem (8).

3 Coupled double integrators

The aim of this paper is to address the minimum switching control problem for a system of n double integrators $x = [x_1, \dots, x_n]^T$, controlled by n switching inputs $u = [u_1, \dots, u_n]^T$,

$$\ddot{x}_j(t) = u_j(t) + k_j, \quad j = 1, \dots, n, \quad (11)$$

where $u_j(t) \in \{-1, 0, 1\}$ and $k_j > 0$. The vector $x(t)$ must satisfy the parallelotopic constraint

$$\|C x(t)\|_\infty \leq 1, \quad (12)$$

where $C \in \mathbb{R}^{n \times n}$ is nonsingular. Notice that the n double integrators (11) are decoupled, but the constraints (12) are coupled. This formulation is equivalent, through a change of coordinates, to n double integrators coupled through a non diagonal input matrix, each of one subject to constraints of the form (3).

For system (11), the minimum-fuel problem amounts to minimizing $J_{f,tot}(u) = \sum_{j=1}^n J_f(u_j)$. Thanks to the decoupling, the optimality condition

$$u_j^*(t) \in \{-1, 0\}, \quad j = 1, \dots, n, \quad (13)$$

still holds, and leads to the optimal fuel cost $J_{f,tot}(u^*) = \sum_{j=1}^n k_j = \|k\|_1$. The minimum switching problem (8) can be generalized to the considered multivariable system, by suitably adapting the cost $J_s(u)$. Since we are interested in reducing as much as possible the number of input transitions

per actuator, this amounts to minimize the maximum $J_s(u_j)$ over all inputs $u_j(t)$, $j = 1, \dots, n$. This corresponds to solving the problem

$$\begin{aligned} \min_u \max_j \quad & J_s(u_j) \\ \text{s.t.} \quad & (11), (12) \\ & u_j(t) \in \{-1, 0\}, \quad j = 1, \dots, n. \end{aligned} \quad (14)$$

Problem (14) is hard to solve if all feasible solutions $x(t)$ are considered. Therefore, by building on the optimal solution of the single-input problem, we restrict our attention to the periodic trajectories given by Proposition 2. To this aim, the trajectory of the j -th integrator is parameterized as

$$\begin{aligned} x_j(t) &= a_j f_j(\lambda_j), \\ \lambda_j &= \text{mod}(t/p_j + \phi_j, 1), \\ a_j &= p_j^2 \gamma_j, \\ \gamma_j &= k_j (1 - k_j)/16, \end{aligned} \quad (15)$$

where a_j is the amplitude, p_j is the period, $\phi_j \in [0, 1]$ is the phase, $\text{mod}(x, y)$ denotes the remainder of x/y , and $f_j(\lambda_j) \in [-1, 1]$ is defined as

$$f_j(\lambda_j) = \begin{cases} 1 - \frac{8}{k_j} (\lambda_j - \frac{k_j}{2})^2 & \text{if } 0 \leq \lambda_j \leq k_j \\ -1 - \frac{8}{k_j-1} (\lambda_j - \frac{k_j+1}{2})^2 & \text{if } k_j < \lambda_j < 1. \end{cases} \quad (16)$$

Notice that (15)-(16) is a parameterization of $\psi^L \cup \psi^U$ in (9)-(10). The input signals u_j are pulse-width modulated with period p_j and duty cycle k_j , and can be expressed as

$$u_j(t) = \begin{cases} -1 & \text{if } 0 \leq \lambda_j \leq k_j \\ 0 & \text{if } k_j < \lambda_j < 1. \end{cases} \quad (17)$$

Since u_j in (17) satisfy (13) and $J_{f,tot}(u) = \|k\|_1$, they are fuel-optimal. Being these signals double-switch periodic, one has $J_s(u_j) = \frac{2}{p_j}$. Moreover, (12) is equivalent to

$$\max_i \max_t \left| \sum_{j=1}^n c_{ij} x_j(t) \right| \leq 1, \quad (18)$$

where the coefficients c_{ij} are the entries of C . By enforcing (15) and replacing (12) by (18), problem (14) becomes

$$\begin{aligned} \min_{p, \phi} \max_j & \frac{2}{p_j} \\ \text{s.t.} & \text{ (15), (18)} \\ & 0 \leq \phi_j < 1 \\ & p_j > 0, \quad j = 1, \dots, n, \end{aligned} \tag{19}$$

where $p = [p_1, \dots, p_n]^T$ and $\phi = [\phi_1, \dots, \phi_n]^T$. So far, the dynamic optimization problem (14) has been converted into a static optimization problem, where the decision variables are p and ϕ . Note, however, that the problem is still hard to solve, being non-convex in these decision variables. Consequently, some simplifying assumptions will be made in order to derive an upper bound to the solution of (19). Let us observe that by (15)

$$\max_t \left| \sum_{j=1}^n c_{ij} x_j(t) \right| \leq \sum_{j=1}^n |c_{ij}| a_j. \tag{20}$$

Hence, (18) can be enforced by imposing $\|\bar{C} a\|_\infty \leq 1$, where $a = [a_1, \dots, a_n]^T$ and \bar{C} is the matrix whose entries are $|c_{ij}|$. From (15), it follows that

$$p_j = \sqrt{a_j / \gamma_j}. \tag{21}$$

By replacing (18) with $\|\bar{C} a\|_\infty \leq 1$ and exploiting (21), problem (19) boils down to

$$\begin{aligned} \min_a \max_j & 2 \sqrt{\frac{\gamma_j}{a_j}} \\ \text{s.t.} & \|\bar{C} a\|_\infty \leq 1 \\ & a_j > 0, \quad j = 1, \dots, n. \end{aligned} \tag{22}$$

By (20), the solution of (22) is an upper bound to that of (19). It turns out that problem (22) can be solved analytically, as stated by the following theorem.

Theorem 1 *A global minimum of problem (22) is attained at*

$$a^* = \frac{1}{\|Q\|_\infty} \Gamma \mathbf{1}, \tag{23}$$

where $\Gamma = \text{diag}(\gamma_1, \dots, \gamma_n)$, $Q = \bar{C}\Gamma$, $\|\cdot\|_\infty$ denotes the matrix infinity norm and $\mathbf{1} = [1, \dots, 1]^T$.

Proof: Let $r = \Gamma^{-1}a$. Then, problem (22) can be rewritten as

$$\begin{aligned} & \min_{\beta, r} \beta \\ & \text{s.t. } \frac{2}{\sqrt{r_j}} \leq \beta \\ & \quad \|Qr\|_\infty \leq 1 \\ & \quad r_j > 0, \quad j = 1, \dots, n. \end{aligned} \tag{24}$$

The statement of the theorem is proven if the feasible solution $r^* = \frac{1}{\|Q\|_\infty} \mathbf{1}$, $\beta^* = 2\sqrt{\|Q\|_\infty}$ is a global minimum for problem (24). Let \hat{r} , $\hat{\beta}$ be another feasible solution of (24). Hence, we get

$$\hat{r}_j \geq \frac{4}{\hat{\beta}^2}, \quad \forall j = 1, \dots, n,$$

and, being $q_{ij} \geq 0$, $\forall i, j$, where q_{ij} denotes the entries of Q , one has

$$1 \geq \sum_{j=1}^n q_{ij} \hat{r}_j \geq \frac{4}{\hat{\beta}^2} \sum_{j=1}^n q_{ij}, \quad \forall i = 1, \dots, n.$$

Hence,

$$\hat{\beta} \geq 2 \sqrt{\max_{i=1, \dots, n} \sum_{j=1}^n q_{ij}} = \beta^*,$$

which concludes the proof. \blacksquare

Since by (23) all the entries of $\Gamma^{-1}a^*$ are equal, it follows from (21) that the periods of the period trajectories resulting from the solution of problem (22) are

$$p_1^* = p_2^* = \dots = p_n^* = \frac{1}{\sqrt{\|Q\|_\infty}}. \tag{25}$$

In the relaxation (22) of problem (19), the additional degrees of freedom provided by the relative phases ϕ_j have not been exploited. In order to find a less conservative relaxation, we enforce directly the property (25) into the original problem (19). This leads to the new relaxed problem

$$\begin{aligned} & \max_{p, \phi} \frac{p_1}{2} \\ & \text{s.t. } (15), (18) \\ & \quad \phi_1 = 0, \quad 0 \leq \phi_j < 1, \quad j = 2, \dots, n \\ & \quad p_1 = p_2 = \dots = p_n > 0, \end{aligned} \tag{26}$$

where $\phi_1 = 0$ has been enforced without loss of generality, since shifting all the phases by the same quantity does not affect the optimal solution of (26).

Theorem 2 *A global minimum of problem (26) is attained at $\phi^* = \arg \min_{\phi} \sigma(\phi)$ and $p_1^* = \frac{1}{\sqrt{\sigma(\phi^*)}}$, where*

$$\sigma(\phi) = \max_i \max_{0 \leq t \leq p_1} \left| \sum_{j=1}^n c_{ij} \gamma_j f(t/p_1 + \phi_j) \right|. \quad (27)$$

Proof: The result easily follows by using (15) and rewriting constraint (18) as $p_1^2 \sigma(\phi) \leq 1$. ■

Due to (20) and (25), the solution of problem (26) is a lower bound to that of (22), while still being an upper bound to that of (19). Notice that $\sigma(\phi)$ in (27) does not depend on the actual value of the period p_1 , because the peak values of the sums of the p_1 -periodic functions $f(t/p_1 + \phi_j)$, evaluated over the period, are independent from the period itself. According to (17), the resulting optimal input signals u_j^* are pulse-width modulated with period $p_j^* = p_1^*$ and phases $\phi_1^* = 0$ and ϕ_j^* for $j = 2, \dots, n$. Finding ϕ^* amounts to solve a crest factor minimization problem, which is known to be a hard optimization problem, being $\sigma(\phi)$ a non convex function. Nevertheless, for low dimensional cases, such as $n = 2$ or $n = 3$, which are of practical interest in many applications, a global minimizer of $\sigma(\phi)$ can be found by numeric search over the free phases ϕ_j .

Example. Let $n = 2$, $k = [0.7, 0.1]^T$ in (11), and

$$C = \begin{bmatrix} \cos(\pi/3) & \sin(\pi/3) \\ -\sin(\pi/3) & \cos(\pi/3) \end{bmatrix},$$

in (12). According to Theorem 1, the solution to (22) is given by $a^* = [0.9257, 0.3967]^T$. From (25), it follows that $p_1^* = p_2^* = 8.4$ and hence the resulting average switching frequency is $J_s(u^*) = 2/p_1^* = 0.238$. Problem (26) is solved using Theorem 2 with $\phi_1 = 0$. The minimizer ϕ_2^* is found numerically through a one-dimensional search. One gets $\phi_2^* = 0.59$ and $p_1^* = p_2^* = 9.53$, which give $J_s(u_j^*) = 2/p_1^* = 0.21$ which is lower than the optimal cost of (22) by approximately 12%. The resulting trajectories $x_1(t)$, $x_2(t)$ of system (11) are shown in the $x_1 x_2$ plane in Fig. 2, together with the set defined by (12) and the box $|x_j| \leq a_j^*$.

4 Minimum switching control law

In this section, it is shown how to control the system to the periodic trajectories previously found, starting from any given initial condition. For

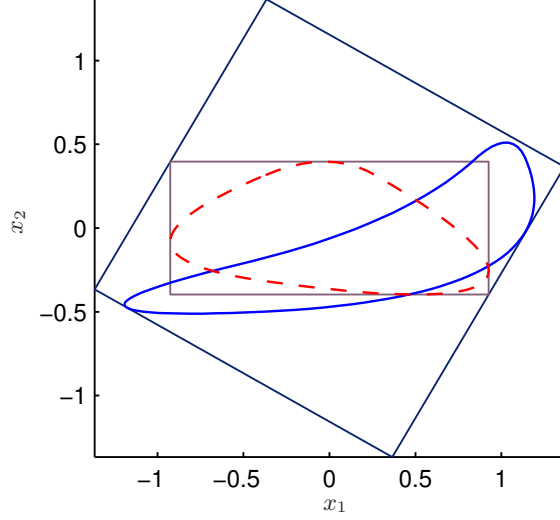


Figure 2: Trajectories in the x_1, x_2 plane from the solutions to (22) (dashed) and (26) (solid), with constraints (12) (outer parallelogram) and $|x_i| \leq a_i^*$ (inner box).

the solution provided by Theorem 1, this amounts to design a control law tracking a limit cycle with prescribed period. For the solution specified by Theorem 2, the control law must also track the phase of the trajectory along the limit cycle.

In order to steer the double integrator (11) to a periodic trajectory of the form (15)-(16), with prescribed period p_j from any initial condition, the fuel-optimal control law (6) is modified as follows

$$u_j(t) = \begin{cases} -1 & \text{if } s(x_j, \dot{x}_j) \geq a_j \\ 0 & \text{if } s(x_j, \dot{x}_j) \leq -a_j \\ u_p & \text{otherwise,} \end{cases} \quad (28)$$

where $u_p = -1$ if $s(x_j, \dot{x}_j) \geq a_j$ occurred more recently than $s(x_j, \dot{x}_j) \leq -a_j$, and $u_p = 0$ otherwise. The resulting closed-loop system consists of the nonlinear system (11), under the relay feedback (28), with $s(x_j, \dot{x}_j)$ defined by (7) and hysteresis a_j . Notice that the switching curve $s(x_j, \dot{x}_j) = a_j$ contains the portion of the curve ψ^U in (10) with $\delta = a_j$, for $\dot{x} > 0$; similarly, $s(x, \dot{x}) = -a_j$ contains the portion of the curve ψ^L in (9) with $\delta = a_j$, for $\dot{x} < 0$. Straightforward phase plane arguments lead to the following result.

Proposition 3 *The perturbed double integrator (11) with the control law (28) converges in finite time to a periodic trajectory of the form (15)-(16), with period p_j given by (21). Moreover, only one switching of the control input is required to reach this trajectory from any initial condition.*

By applying for each input signal $u_j(t)$ of system (11) the control law (28) with $a_j = a_j^*$ given by Theorem 1, the periodic trajectories (15) with period p_j^* in (25) are reached in finite time with one switching per input, from any initial condition.

Besides the relationship between the hysteresis of the relay element and the period of the limit cycle, a relationship between a variation of the hysteresis width and a corresponding phase shift does indeed exist. Therefore, the approach proposed hereafter is to steer both the period and the phase of the closed-loop trajectory to p_j^* and ϕ_j^* resulting from Theorem 2, by using a time-varying hysteresis defined by two parameters $a_j^U(t)$ and $a_j^L(t)$. More specifically, the following procedure is proposed: upon reaching of a switching curve, the parameter defining the offset of the opposite switching curve is updated, to enforce a cycle whose duration is designed to steer both the phase and the period to the prescribed values. To this purpose, the control law (28) is modified as

$$u_j(t) = \begin{cases} -1 & \text{if } s(x_j, \dot{x}_j) \geq a_j^U(t) \\ 0 & \text{if } s(x_j, \dot{x}_j) \leq -a_j^L(t) \\ u_p & \text{otherwise,} \end{cases} \quad (29)$$

where $u_p = -1$ if $s(x_j, \dot{x}_j) \geq a_j^U(t)$ occurred more recently than $s(x_j, \dot{x}_j) \leq -a_j^L(t)$, and $u_p = 0$ otherwise, with $a_j^L(t) + a_j^U(t) > 0$. The time-varying parameters are designed as explained next. Hereafter, for the sake of exposition, the subscript j denoting the input channel will be dropped.

Let $\{z_m^L\}$, $\{z_m^U\}$ denote two sequences of increasing time instants at which the trajectory reaches the switching curves of the control law (29). Without loss of generality, let us consider $u(t_0) = 0$ (the case $u(t_0) = -1$ being analogous) and construct a sequence $\{z_l\}$ of increasing time instants as $\{z_l\} = \{z_1^U, z_1^L, z_2^U, z_2^L, \dots\}$. The proposed approach is to update $a^U(t)$ and $a^L(t)$ in (29) at times z_m^L and z_m^U , respectively. To this aim, let us define a sequence $\{d_l\}$ such that

$$\begin{aligned} a^L(t) &= d_{2m-1} \quad \text{for } t \in [z_{2m-1}, z_{2m+1}), \\ a^U(t) &= d_{2m} \quad \text{for } t \in [z_{2m}, z_{2m+2}). \end{aligned} \quad (30)$$

Notice that the offset of a switching curve is updated when the trajectory is not lying on the same curve.

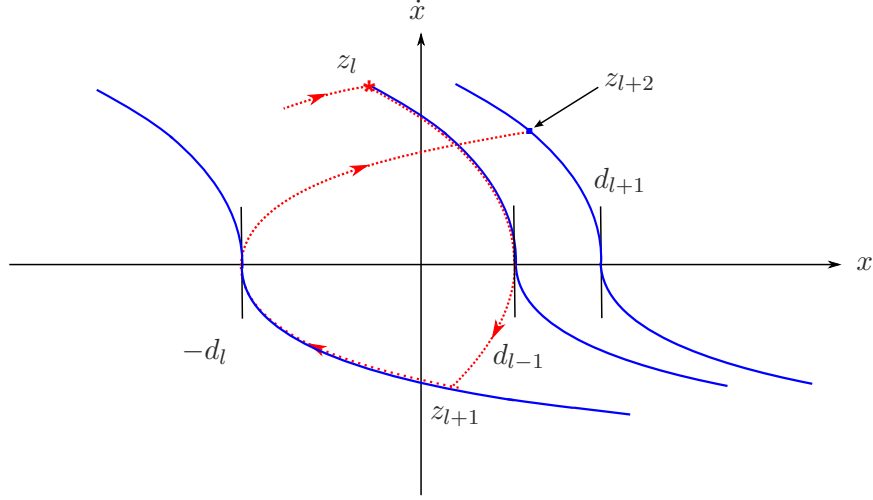


Figure 3: Scheme for the computation of the event times: switching curves (solid) and example of a closed-loop trajectory (dotted).

The sequence $\{z_l\}$ depends on the application of the control law (29) to system (11) and hence on the particular choice of the update sequence $\{d_l\}$ in (30). The controlled evolution of the system is illustrated in Fig. 3, where the state trajectory (dotted) reaches the time-varying switching curves (solid) at times z_l , z_{l+1} and z_{l+2} . The event times can be computed iteratively according to

$$z_{l+1} = z_l + \frac{|\dot{x}(z_{l+1})| + |\dot{x}(z_l)|}{q(z_l)}, \quad (31)$$

where $q(z_l) = |k + u(z_l)|$ and the velocity $|\dot{x}(z_{l+1})|$ is given by

$$|\dot{x}(z_{l+1})| = 4\sqrt{2\gamma(d_l + d_{l-1})}. \quad (32)$$

From the previous observations, it follows that the objective of driving the system to a steady state periodic solution in the form (15)-(16), with prescribed period p and phase ϕ , can be recast in terms of the design of the sequence $\{d_l\}$.

Theorem 3 *Let $a = p^2\gamma$ and define the sequence $\{d_l\}$ as*

$$d_0 = a, \quad (33)$$

$$d_l = a \left(1 + 4\Delta\phi_l + 2\Delta\phi_l^2 \right), \quad (34)$$

where

$$\Delta\phi_l = \text{mod} \left(\frac{\bar{z}_{l+2} - \hat{z}_{l+2}}{p} + \frac{1}{2}, 1 \right) - \frac{1}{2}, \quad (35)$$

$$\hat{z}_{l+2} = z_l + \frac{|\dot{x}(z_l)|}{q(z_l)} + \frac{q(z_l)}{2}p + \frac{\sqrt{2}}{4} \sqrt{p^2 + \frac{d_{l-1}}{\gamma}}, \quad (36)$$

and the variables $\{\bar{z}_l\}$ are defined according to

$$\begin{aligned} \bar{z}_{2m-1} &= -\phi p, \\ \bar{z}_{2m} &= (k - \phi) p, \end{aligned} \quad (37)$$

for $m \in \mathbb{N}$. Then, the solution of system (11) with the control law (29)-(30) converges in finite time to the periodic trajectory (15)-(16) with period p and phase ϕ . Moreover, only three switchings of the control input are required to reach this trajectory from any initial condition.

Proof: Under the assumption that $u(t_0) = 0$ (the reasoning is the same if $u(t_0) = -1$), the closed-loop system trajectory will reach the curve $s(x, \dot{x}) = d_0 = a$ at a certain time z_1 , at which the input switches to $u(z_1) = -1$. Without loss of generality, let $z_1 = 0$. Since $q(z_1) = 1 - k$, (33) and (36) give

$$\hat{z}_3 = \frac{\dot{x}(z_1)}{1 - k} + \left(1 - \frac{k}{2}\right)p.$$

By using (31)-(32), it is possible to check that \hat{z}_3 represents the time at which the trajectory of the closed-loop system would reach again the curve $s(x, \dot{x}) = a$ if one enforced $d_1 = d_2 = a$ in (29)-(30). Being $\bar{z}_3 = -\phi p$,

$$\Delta\phi_1 = h - \phi - \frac{|\dot{x}(z_1)|}{p(1 - k)} + \frac{k}{2}, \quad (38)$$

for some $h \in \mathbb{Z}$. By using d_1 from (34), with $\Delta\phi_1$ given by (38), the procedure is repeated at time z_2 . After simple manipulations, one obtains

$$\begin{aligned} \hat{z}_4 &= \frac{|\dot{x}(z_1)|}{1 - k} + p(1 + \Delta\phi_1) + \frac{k}{2}p, \\ \bar{z}_4 &= (k - \phi)p, \\ \Delta\phi_2 &= \text{mod} \left(-\frac{1}{2} - h, 1 \right) - \frac{1}{2} = 0, \end{aligned}$$

and hence $d_2 = a$. By induction, it can be easily verified that $\Delta\phi_l = 0$ and $d_l = a$, $\forall l \geq 2$, for any $\dot{x}(z_1)$. Hence, by (30), $a^U(t) = a^L(t) = a$,

for all $t \geq z_3$. From Proposition 3, one has that the closed-loop trajectory converges to a solution of the form (15)-(16) with period p . Moreover, from (31)-(32) it follows that the sequence of switching times z_l satisfies

$$\text{mod} \left(\frac{\bar{z}_l - z_l}{p} + \frac{1}{2}, 1 \right) - \frac{1}{2} = 0, \quad \forall l \geq 4. \quad (39)$$

On the other hand, the switching times of the periodic solution (15)-(16) with given phase ϕ occur at time instants \tilde{t} such that either $\text{mod}(\tilde{t}/p + \phi, 1) = 0$ or $\text{mod}(\tilde{t}/p + \phi, 1) = k$. These equations lead to $\tilde{t} = z_{2m-1}$ and $\tilde{t} = z_{2m}$ in (37), respectively. Therefore, (39) guarantees that, for all $t \geq z_4$, the switching times of the closed-loop trajectory coincide with those of the periodic solution (15)-(16), with desired period p and phase ϕ . Finally, since by (35) $-1/2 \leq \Delta\phi_1 < 1/2$, which implies $d_1 \geq -1/2 a$ by (34), one has that $a^L(t) + a^U(t) > 0 \forall t$, as it is required for the control law (29) to be well defined. This concludes the proof. \blacksquare

By applying for each input signal $u_j(t)$ of system (11) the control law (29)-(30), with the input sequence $\{a_l\}$ chosen as in Theorem 3 and $p_j = p_j^*$, $\phi_j = \phi_j^*$ given by Theorem 2, the periodic trajectories (15) with period p_j^* and phase ϕ_j^* are reached in finite time with three switchings per input channel, from any initial condition.

5 Attitude control application

Consider a 2000 kg spacecraft on a geostationary orbit, whose propulsion system consists of the four orbit control thruster O1-O4 and the six attitude control thruster A1-A6 depicted in Fig. 4. Thrusters A1-A3 produce opposite torques with respect to A4-A6. During station-keeping (orbit control) maneuvers, a large disturbance torque, with respect to environmental perturbations, is generated due to misalignment of thrusters O1-O4 with respect to the spacecraft center of mass. Because a station-keeping maneuver requires to fire two orbit control thrusters in sequence, to correct for orbital inclination and longitude errors, such disturbance is piecewise constant. In order to maintain the desired Earth-pointing orientation, it must be compensated using thrusters A1-A6. In the following, the proposed control strategy is applied to this purpose, and compared to the MPC scheme developed in [14], based on a finite horizon reformulation of the optimal control problem (14), which requires the solution of a mixed-integer linear program (MILP).

The simulation environment relies on the fully nonlinear attitude dynamic

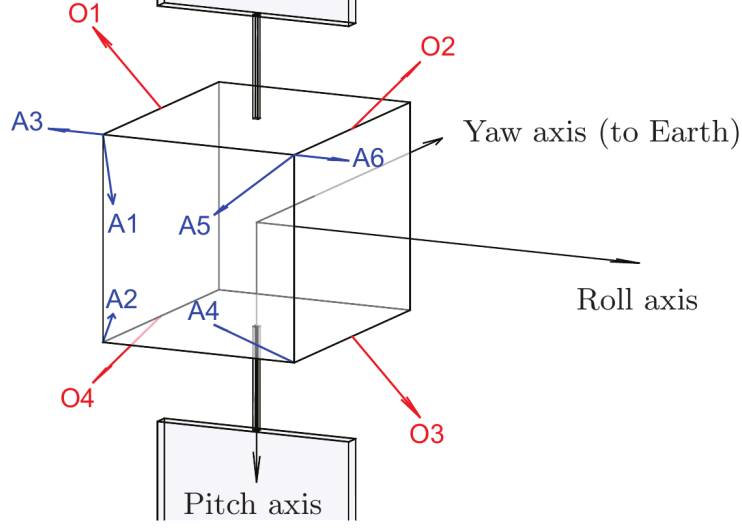


Figure 4: Thruster configuration.

model, see e.g. [15], while for the purpose of control design the attitude error dynamics are approximated by $\ddot{\theta} = I_M^{-1}(Bu + \tau)$, where θ expresses the roll, pitch and yaw errors, I_M is the spacecraft inertia matrix, B maps the thruster activation command $u \in \{-1, 0, 1\}^3$ into the corresponding torque and τ is the disturbance torque. In the considered problem $I_M = \text{diag}(1.9, 1.47, 1.55) \cdot 10^3$,

$$B = \begin{bmatrix} -2 & 2 & 0 \\ 2 & 2 & -1.9 \\ 0 & 0 & 1.5 \end{bmatrix} \cdot 10^{-3},$$

$\tau = [1.2, 0.7, 1]^T$ mNm during the first half of the station-keeping maneuver, $\tau = [0.2, 1.4, 0.5]^T$ mNm during the second half, and the maneuver lasts for 3000 s. The required attitude control accuracy is $\|\theta\|_\infty \leq 0.5$ mrad. The above model can be cast in the form (11)-(12) by adopting the coordinate transformation $x = B^{-1}I_M\theta$ and setting $C = I_M^{-1}B/(5 \cdot 10^{-4})$. An extended Kalman filter takes care of estimating the disturbance torque from attitude and rate measurements. More details on the considered navigation system can be found in [14]. The solutions provided by Theorems 1 and 2 are evaluated twice during the maneuver, to account for the impulsive variation of the disturbance at $t = 1500$ s.

In Fig. 5, the attitude error trajectories resulting from the application of

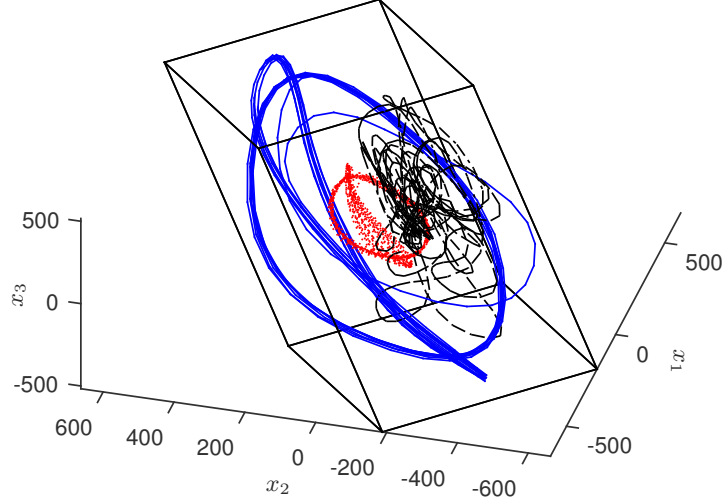


Figure 5: Trajectories in the x space for the MS1 (red, dotted), MS2 (blue, solid) and MPC (black, dash-dotted) control schemes, with constraints (12).

the control law (28), exploiting the solution of Theorem 1 (MS1), and of the control law (29), making use of Theorem 2 (MS2), are compared to that obtained by applying the MPC scheme. It can be seen that the three approaches succeed in keeping the tracking error within the bounds (outer parallelepiped), except for a negligible constraint violation by the MS2 approach during the short transient following the impulsive disturbance variation, due to the requirement to track a new reference phase. The fuel consumption (evaluated in terms of the sum of the actuator firing times) and the maximum actuator switching frequency are reported in Table 1. While the former is approximately the same for the three solutions, the latter is higher for the MPC law. In particular, the application of the MS2 scheme requires a much lower switching frequency, which translates into an increased lifetime of the attitude control thrusters. The superior performance of the proposed approach, with respect to the MPC scheme, is explained by the fact that the MPC optimization problem has to be solved over a finite prediction horizon, in order to retain the computational feasibility of the receding horizon strategy. In fact, the time needed to solve the MILP problem within the MPC scheme is of the same order as that required to evaluate the solution of Theorem 2 through a two-dimensional search on ϕ_2 and ϕ_3 . However, the MILP problem has to be solved at every sampling instant, while the solution of Theorem 2 has to be computed only twice per station-keeping maneuver

Table 1: Control system performance

Parameter	MPC	MS1	MS2
Firing time [s]	4520	4478	4487
Switching frequency [Hz]	0.028	0.020	0.012

(i.e., when the disturbance torque changes).

6 Conclusions

The minimum switching control problem has been addressed for a system of coupled double integrators with on-off input signals, in the presence of a constant disturbance term. Two suboptimal solutions have been presented, which provide upper bounds on the number of input transitions of the resulting steady state limit cycles. A control law driving the system to these limit cycles in finite time has been derived. Simulation results of an attitude control case study have shown that exploiting the relative phases of the periodic trajectories of each state variable provides a significant reduction of the actuator switching frequency.

Several aspects of the considered problem still remain to be investigated. It is not clear how to tackle the minimum switching problem without parameterizing the trajectory in the same form as the optimal solution for the SISO case. A further relaxation would be the removal of the assumption that the considered trajectories are unimodal limit cycles: at least in principle, oscillations resulting from more complex combination of the actuator switchings, may result in a lower number of input transitions. Another subject of ongoing investigation is the application of the proposed controller to the case of coupled double integrators with time-varying disturbances. This would require to evaluate the reference periodic trajectories online, which appears to be feasible whenever the control bandwidth is large compared to the disturbance variation rate.

Acknowledgement

The authors would like to thank prof. Antonio Vicino for useful discussions and suggestions.

References

- [1] A. Feuer, G. Goodwin, and M. Salgado, “Potential benefits of hybrid control for linear time invariant plants,” in *Proceedings of the 1997 American Control Conference*, Albuquerque, NM, June 1997, pp. 2790–2794.
- [2] K. Lau and R. H. Middleton, “Switched integrator control schemes for integrating plants,” *European Journal of Control*, vol. 9, no. 6, pp. 539–559, 2003.
- [3] S. Azuma and T. Sugie, “Optimal dynamic quantizers for discrete-valued input control,” *Automatica*, vol. 44, no. 2, pp. 396 – 406, 2008.
- [4] K. J. Åström, “Oscillations in systems with relay feedback,” in *Adaptive Control, Filtering, and Signal Processing*, K. J. Åström, G. C. Goodwin, and P. R. Kumar, Eds. Springer, 1995, pp. 1–25.
- [5] S. Nugent and R. Kavanagh, “Self and forced oscillations in multivariable relay control systems,” *Automatica*, vol. 5, no. 4, pp. 519–527, 1969.
- [6] A. Loh and V. Vasnani, “Necessary conditions for limit cycles in multiloop relay systems,” *IEE Proceedings - Control Theory and Applications*, vol. 141, no. 3, pp. 163–168, 1994.
- [7] I. Boiko, A. Pisano, and E. Usai, “Frequency-domain analysis of self-excited oscillations for a class of multivariable relay systems,” in *Proceedings of 2013 European Control Conference*, Zurich, Switzerland, July 2013, pp. 4287–4292.
- [8] J. M. Gonçalves, “Regions of stability for limit cycle oscillations in piecewise linear systems,” *IEEE Transactions on Automatic Control*, vol. 50, no. 11, pp. 1877–1882, 2005.
- [9] D. Flieller, P. Riedinger, and J.-P. Louis, “Computation and stability of limit cycles in hybrid systems,” *Nonlinear Analysis: Theory, Methods & Applications*, vol. 64, no. 2, pp. 352–367, 2006.
- [10] D. Patino, P. Riedinger, and C. Iung, “Practical optimal state feedback control law for continuous-time switched affine systems with cyclic steady state,” *International Journal of Control*, vol. 82, no. 7, pp. 1357–1376, 2009.

- [11] X. Ding, Y. Wardi, D. Taylor, and M. Egerstedt, “Optimization of switched-mode systems with switching costs,” in *Proceeding of 2008 American Control Conference*, Seattle, WA, June 2008, pp. 3965–3970.
- [12] H. Deng, L. Larsen, J. Stoustrup, and H. Rasmussen, “Control of systems with costs related to switching: applications to air-condition systems,” in *Proceedings of 18th IEEE Conference on Control Applications*, San Petersburg, Russia, July 2009, pp. 554–559.
- [13] B. Solberg, P. Andersen, J. M. Maciejowski, and J. Stoustrup, “Optimal switching control of burner setting for a compact marine boiler design,” *Control Engineering Practice*, vol. 18, no. 6, pp. 665–675, 2010.
- [14] M. Leomanni, A. Garulli, A. Giannitrapani, and F. Scortecci, “All-electric spacecraft precision pointing using model predictive control,” *Journal of Guidance, Control and Dynamics*, vol. 38, no. 1, pp. 161–168, 2015.
- [15] M. H. Kaplan, *Modern spacecraft dynamics and control*. New York: John Wiley and Sons, 1976.
- [16] M. Coletti, A. Grubisic, C. Collingwood, and S. Gabriel, “Solar electric propulsion subsystem architecture for an all-electric spacecraft,” in *Advances in Spacecraft Technologies*, J. Hall, Ed. InTech, 2011, pp. 123–138.
- [17] M. Athans and P. L. Falb, *Optimal control: an introduction to the theory and its applications*. Courier Dover Publications, 2006.